Inorg. Chem. **2007**, *46*, 2854–2863

Ruthenium(II) Complexes with Improved Photophysical Properties Based on Planar 4′-(2-Pyrimidinyl)-2,2′:6′,2″-terpyridine Ligands

Yuan-Qing Fang,[†] Nicholas J. Taylor,[†] François Laverdière,[†] Garry S. Hanan,*[,†] Frédérique Loiseau,[‡] Francesco Nastasi,[‡] Sebastiano Campagna,*[,‡] Hélène Nierengarten,[§] Emmanuelle Leize-Wagner,[||] and Alain Van Dorsselaer[§]

Department of Chemistry, University of Waterloo, Waterloo, Ontario, Canada N2L 3G1, Département de Chimie, Université de Montréal, Canada H3T 1J4, Dipartimento di Chimica Inorganica, Chimica Analitica e Chimica Fisica, Università di Messina, 98166 Messina, Italy, UMR 7509, LSMBO-ECPM, 67087 Strasbourg, France, and Laboratoire de Dynamique et Structure Moleculaire par Spectrometrie de Masse-ISIS, CNRS-Université de Strasbourg, 67083 Strasbourg, France

Received November 28, 2006

A series of new tridentate polypyridine ligands, made of terpyridine chelating subunits connected to various substituted 2-pyrimidinyl groups, and their homoleptic and heteroleptic Ru(II) complexes have been prepared and characterized. The new metal complexes have general formulas $[(R\text{-pm-tpy})Ru(tpy)]^{2+}$ and $[Ru(tpy\text{-pm-}R)_2]^{2+}$ (tpy = 2,2′:6′,2″-terpyridine; R-pm-tpy = 4′-(2-pyrimidinyl)-2,2′:6′,2″-terpyridine with R = H, methyl, phenyl, perfluorophenyl, chloride, and cyanide). Two of the new metal complexes have also been characterized by X-ray analysis. In all the R-pm-tpy ligands, the pyrimidinyl and terpyridyl groups are coplanar, allowing an extended delocalization of acceptor orbital of the metal-to-ligand charge-transfer (MLCT) excited state. The absorption spectra, redox behavior, and luminescence properties of the new Ru(II) complexes have been investigated. In particular, the photophysical properties of these species are significantly better compared to those of $[Ru(tpy)_2]^{2+}$ and well comparable with those of the best emitters of Ru(II) polypyridine family containing tridentate ligands. Reasons for the improved photophysical properties lie at the same time in an enhanced MLCT-MC (MC = metal centered) energy gap and in a reduced difference between the minima of the excited and ground states potential energy surfaces. The enhanced MLCT-MC energy gap leads to diminished efficiency of the thermally activated pathway for the radiationless process, whereas the similarity in ground and excited-state geometries causes reduced Franck Condon factors for the direct radiationless decay from the MLCT state to the ground state of the new complexes in comparison with $[Ru(tpy)_2]^{2+}$ and similar species.

Introduction

Ruthenium(II) polypyridine complexes have played important roles in several areas of research connected with solar energy conversion over the last three decades.[1] The prototype of this class of compound, $[Ru(bpy)_3]^{2+}$ (bpy = 2,2′-bipyridine), is one of the most studied metal-containing species due to a combination of high photostability and interesting electrochemical and photophysical properties.[2] However, for several applications (for example, for vectorial energy and electron transfer in "molecular wires"[3]), the Ru(II) complex of the tridentate ligand tpy (tpy = 2,2′:6′,2″-terpyridine), i.e. $[Ru(tpy)_2]^{2+}$, is structurally more appealing than $[Ru(bpy)_3]^{2+}$. Furthermore, synthesizing discrete polynuclear complexes based on $[Ru(bpy)_3]^{2+}$ subunits is hampered by the mixtures of diasteromers that form due to its Δ and Λ enantiomers and by the *fac* and *mer* isomers generated by monosubstituted bpy ligands.[4] Symmetrically substituted tridentate polypyridine ligands would overcome these structural problems; however, their Ru(II) complexes, e.g., $[Ru(tpy)_2]^{2+}$ and derivatives, have much less useful photophysical properties than $[Ru(bpy)_3]^{2+}$.[2] This is due primarily to the weaker ligand field strength of tpy, which leads to lower

* To whom correspondence should be addressed. E-mail: garry.hanan@umontreal.ca (G.S.H.), campagna@unime.it (S.C.).
[†] University of Waterloo and Université de Montréal.
[‡] Università di Messina.
[§] UMR 7509, LSMBO-ECPM.
[||] CNRS-Université de Strasbourg.

10.1021/ic0622609 CCC: $37.00
Published on Web 02/16/2007

energy metal-centered (MC) states as compared to Ru(II) complexes of bpy. Thus, there is sufficient energy at room temperature (rt) to efficiently populate the MC states from the MLCT states and lead to fast deactivation of the excited-state by nonradiative processes.

Much effort has been devoted to the design and synthesis of tridentate polypyridine ligands that lead to Ru(II) complexes with more interesting photophysical properties.[5] For example, the use of ligands containing electron withdrawing and donor substituents on tpy increase the gap between the ^{3}MLCT and the ^{3}MC states.[6] One can also modify the terpyridine directly, by replacing the pyridines with other heterocyclic rings.[7] Another example is the extension of the π^* orbital by the appropriate substituent, which increases the delocalization of the acceptor ligand of the MLCT excited-state leading to reduced Franck−Condon factors for nonradiative decay as a consequence of similarity between the minima of the ground and excited states potential energy surfaces. Within this latter approach, species based on ethynyl-substituted tpy possess interesting photophysical properties.[8]

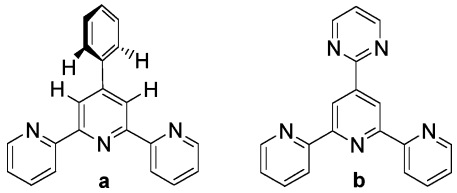

Figure 1. Ligands with nonplanar (a) 4′-phenyl-tpy and planar (b) 4′-(2-pyrimidyl)-tpy aromatic rings in the 4′-position of tpy.

An extension of this approach could make use of aryl-substituted tpy's as they are very good candidates for electron delocalization by π-conjugation. However, the results from photophysical measurements are quite disappointing when a phenyl group is introduced into the 4′-position of tpy, with $[Ru(Ph\text{-}tpy)_2]^{2+}$ (**5**; Ph-tpy = 4′-phenyl-2,2′:6′-2″-terpyridine) having a lifetime of only 1.0 ns at room temperature.[6] Although longer than the lifetime of $[Ru(tpy)_2]^{2+}$(**4**) in the same conditions (250 ps[3b]), the improvement in the photophysical properties were in fact limited. The limited improvement in the photophysical properties of **5** are due to a twist between the phenyl and central pyridine rings caused by the unfavorable interaction between the four protons adjacent to the interannular bond (Figure 1a). Computational results for the angle between planes in biphenyl is around 45°,[9] and the statistical result for analogous fragments from crystal structures database shows that most frequent value is 20−30°.[10] The nonplanarity between terpyridyl and phenyl rings led to mismatch between ground and excited states geometries, minimizing the effect of increased delocalization.

In order to increase the π-conjugation between the aromatic ring and the tpy and obtain planarization also in the ground state, the phenyl ring could be replaced with other aromatic rings. By replacing the phenyl ring with a 2-pyrimidyl ring, the carbon atoms adjacent to the interannular bond are replaced with nitrogen atoms and the rings should lie coplanar, lowering the energy of π^* orbitals due to better π-conjugation.[11] The pyrimidinyl subunits increase the available area for π-conjugation between the heterocyclic rings of the tpy, while at the same time maintaining planarity for maximum π-delocalization (Figure 1). Herein we report on the synthesis and characterization of this new family of ligand and their Ru(II) complexes. The effect of introducing the 2-pyrimidinyl subunits on the photophysical properties of the $[Ru(tpy)_2]^{2+}$ chromophore is also investigated. The new species synthesized and studied are the hetero- and homoleptic compounds $[(tpy\text{-}pm\text{-}R)Ru(tpy)]^{2+}$ and [Ru(tpy-

(1) (a) Balzani, V.; Scandola, F. *Supramolecular Photochemistry*; Horwood: Chichester, 1991. (b) Balzani, V.; De Cola, L. *Supramolecular Chemistry*; Kluwer: Dordrecht, 1992. (c) Balzani, V.; Credi, A.; Venturi, M. *Molecular Devices and Machines*; Wiley-VCH: Weinheim, 2003. (d) Scandola, F.; Chiorboli, C.; Indelli, M. T.; Rampi, M. A. In *Electron Transfer in Chemistry*; Balzani, V., Ed.; VCH-Wiley: 2001; Vol. 3, p 337. (e) Sun, L.; Hammarström, L.; Akermark, B.; Styring, S. *Chem. Soc. Rev.* **2001**, *30*, 36−49. (f) Wang, X.; Guerzo, A.; Baitalik, S.; Simon, G.; Shaw, G. B.; Chen, L. X.; Schmehl, R. *Photosynth. Res.* **2006**, *87*, 83. (g) Liu, Y.; DeNicola, A.; Ziessel, R.; Schanze, K. S. *J. Phys. Chem. A* **2003**, *107*, 3476. (h) Alstrum-Acevedo, J. H.; Brennaman, M. K.; Meyer, T. J. *Inorg. Chem.* **2005**, *44*, 6802. (i) Browne, W. R.; O'Boyle, N. M.; McGarvey, J. J.; Vos, J. G. *Chem. Soc. Rev.* **2005**, *34*, 641. (l) Balzani, V.; Clemente-Léon, M.; Credi, A.; Ferrer, B.; Venturi, M.; Flood, A. H.; Stoddart, J. F. *Proc. Natl. Acad. Sci. U.S.A.* **2006**, *103*, 1178. (m) Kuang, D.; Ito, S.; Wenger, B.; Klein, C.; Moser, J.-E.; Humphry-Baker, R.; Zakeeruddin, S. M.; Gratzel, M. *J. Am. Chem. Soc.* **2006**, *128*, 4146 and references therein.

(2) (a) Meyer, T. J. *Pure Appl. Chem.* **1986**, *58*, 1193. (b) Juris, A.; Balzani, V.; Barigelletti, F.; Campagna, S.; Belser, P.; Von Zelewsky, A. *Coord. Chem. Rev.* **1988**, *84*, 85.

(3) (a) Baranoff, E.; Collin, J.-P.; Flamigni, L. Sauvage, J.-P. *Chem. Soc. Rev.* **2004**, *33*, 147. (b) Sauvage, J. P.; Collin, J. P.; Chambron, J. C.; Guillerez, S.; Coudret, C.; Balzani, V.; Barigelletti, F.; De, Cola, L.; Flamigni, L. *Chem. Rev.* **1994**, *94*, 993−1019. (c) Patoux, C.; Launay, J.-P.; Beley, M.; Chodorowski-Kimmes, S.; Collin, J.-P.; James, S. Sauvage, J.-P. *J. Am. Chem. Soc.* **1998**, *120*, 3717. (d) Hammarström, L.; Barigelletti, F.; Flamigni, L.; Indelli, M. T.; Armaroli, N.; Calogero, G.; Guardigli, M.; Sour, A.; Collin, J.-P.; Sauvage, J.-P. *J. Phys. Chem. A* **1997**, *101*, 9061. (e) Balzani, V.; Juris, A.; Venturi, M.; Campagna, S.; Serroni, S. *Chem. Rev.* **1996**, *96*, 759. (f) *Top. Curr. Chem.* **2005**, *257*, special issue entitled *Molecular Wires*, De Cola, L., Ed.

(4) (a) Von Zelewsky, A. *Stereochemistry of coordination compounds*; John Wiley & Sons Ltd.: New York, 1996. (b) Balzani, V.; Juris, A.; Venturi, M.; Campagna, S.; Serroni, S. *Chem. Rev.* **1996**, *96*, 759.

(5) (a) Harriman, A.; Ziessel, R. *Chem. Comm.* **1996**, 1707. (b) Benniston, A. C.; Harriman, A.; Grosshenny, V.; Ziessel, R. *New. J. Chem.* **1997**, *21*, 405. (c) El-Ghayoury, A.; Harriman, A.; Khatyr, A.; Ziessel, R. *J. Phys. Chem. A* **2000**, *104*, 1512. (d) Polson, M. I. J.; Medlycott, E. A.; Mikelsons, L.; Taylor, N. J.; Watanabe, M.; Tanaka, Y.; Loiseau, F.; Passalaqua, R.; Campagna, S. *Chem. Eur. J.* **2004**, *10*, 3640. (e) Medlycott, E. A.; Hanan, G. S. *Chem. Soc. Rev.* **2005**, *34*, 133. (f) Medlycott, E. A.; Hanan, G. S. *Coord. Chem. Rev.* **2006**, *250*, 1763 and references therein.

(6) Maestri, M.; Armaroli, N.; Balzani, V.; Constable, E. C.; Thompson, A. M. W. C. *Inorg. Chem.* **1995**, *34*, 2759.

(7) (a) Abrahamsson, M.; Jäger, M.; Osterman, T.; Eriksson, L.; Persson, P.; Becker, H.-C.; Johansson, O.; Hammarström, L. *J. Am. Chem. Soc.* **2006**, *128*, 12616. (b) Medlycott, E. A.; Hanan, G. S. *Inorg. Chem. Commun.* **2006**, in press. (c) Medlycott, E. A.; Hanan, G. S.; Loiseau, F.; Campagna, S. *Chem. Eur. J.* **2006**, accepted for publication. (d) Duati, M.; Tasca, S.; Lynch, F. C.; Bohlen, H.; Vos, J. G.; Stagni, S.; Ward, M. D. *Inorg. Chem.* **2003**, *42*, 8377. (e) Liegghio, R.; Potvin, P. G.; Lever, A. B. P. *Inorg. Chem.* **2001**, *40*, 5485.

(8) (a) Benniston, A. C.; Grosshenny, V.; Harriman, A.; Ziessel, R. *Angew. Chem., Int. Ed.* **1994**, *33*, 1884. (b) Hissler, M.; El-Ghayoury, A.; Harriman, A.; Ziessel, R. *Angew. Chem., Int. Ed.* **1998**, *37*, 1717. (c) El-Ghayoury, A.; Harriman, A.; Khatyr, A.; Ziessel, R. *Angew. Chem.* **2000**, *112*, 191. (d) Benniston, A. C.; Harriman, A. Li, P.*; Sams, C. A. J. Am. Chem. Soc.* **2005**, *127*, 2553. (e) Barbieri, A.; Ventura, B.; Barigelletti, F.; De Nicola, A.; Quesada, M.; Ziessel, R. *Inorg. Chem.* **2004**, *43*, 7359. (f) Benniston, A. C.; Harriman, A. *Inorg. Chim. Acta* **2006**, 359, 753.

(9) Goller, A.; Grummt, U. W. *Chem. Phys. Lett.* **2000**, *321*, 399.

(10) Brock, C. P.; Minton, R. P. *J. Am. Chem. Soc.* **1989**, *111*, 4586.

(11) Gompper, R.; Mair, H. J.; Polborn, K. *Synthesis* **1997**, 696.

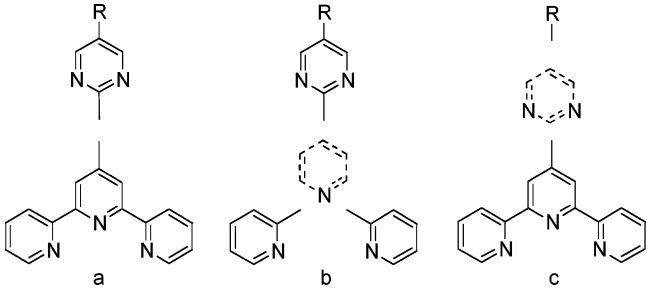

Figure 2. Different approaches to the 4′-(2-pyrimidyl)-2,2′:6′,2″-terpyridine ligands: (a) C−C bond-forming, (b) pyridine ring-forming, and (c) pyrimidine ring-forming reactions.

pm-R)$_2$]$^{2+}$, respectively (tpy = 2,2′:6′,2″-terpyridine; tpy-pm-R = 4′-(2-pyrimidyl)-2,2′:6′,2″-terpyridine and R = H, Me, phenyl, perfluorophenyl, Cl, and CN). Preliminary data concerning complexes **2** were previously communicated.[12]

Results and Discussion

Two different synthetic methods could be used to form the tpy-pm-R ligands: carbon−carbon bond forming reactions (Figure 2a)[13] or heterocyclic ring forming reactions (Figure 2b).[14] The introduction of aromatic rings into the 4′-position of tpy by C−C bond forming reactions would make use of 4′-halogenated-tpy and 2-pyrimidyl substituted organometallic reagents (Figure 2a). The successful introduction of phenyl[15] and alkyne[8] groups into the 4′-position of tpy strongly support such an approach; however, the 2-pyrimidyl rings could not be functionalized further without difficulty. Although ring forming the central pyridine of the terpyridine is a feasible approach (Figure 2b), the synthesis of variably substituted 2-formyl-pyrimidines would not be straightforward. Thus, a pyrimidine ring forming reaction was envisaged,[11] whereby 4′-terpyridylamidine would be reacted with a variety of vinamidium salts to give the tpy-pm-R ligands (Figure 2c).

The starting point was the 4′-cyanoterpyridine moiety, which was converted into 4′-terpyridylamidine hydrochloride **7** by forming the imidate intermediate with NaOMe, followed by the addition of NH_4Cl (Scheme 1).[16]

A series of 2-substituted trimethinium (vinamidium) salts **8a**−**f** was prepared with either hexafluorophosphate (PF_6) or perchlorate (ClO_4) as counteranions. The series included the standard for Hammett parameter analyses, H (**a**),[17] an

Scheme 1. In Situ Two-Step Synthesis of 4′-Terpyridylamidine Hydrochloride **7**

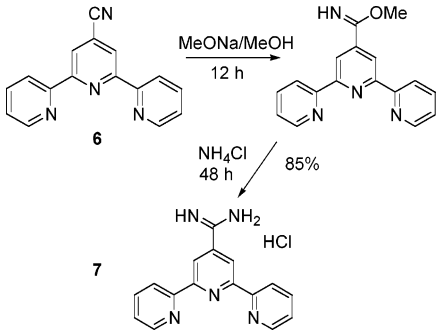

Scheme 2. Synthesis of 4′-(2-Pyrimidyl)tpy Ligands 1 from **7** and **8**

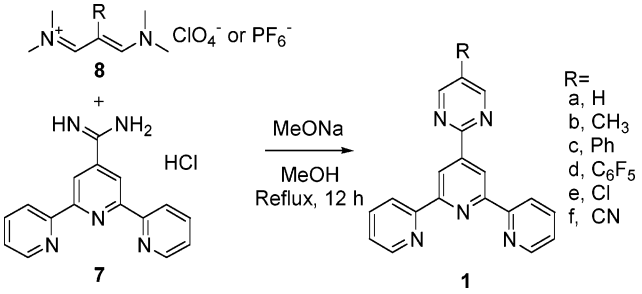

electron-donating Me group (**b**),[18] a phenyl group (**c**),[19] and three electron-withdrawing groups: C_6F_5 (pentafluorophenyl, **d**),[19] Cl (**e**),[19] and CN (**f**).[20]

It was found that the reactions to form **1** from 4′-terpyridylamidine hydrochloride **7** and the vinamidine salts **8** were very facile (Scheme 2). In the presence of sodium methoxide in methanolic solution, the reactions proceed rapidly with release of dimethylamide. Products **1** are only slightly soluble in methanol and precipitate from solution as the reactions proceed. Filtration and recrystallization from ethanol affords analytically pure products in reasonable yields (71−85%) without chromatographic purification, except for **1a** in which the yield was quite low (30%).

With the ligands in hand, both the heteroleptic ([(tpy)Ru(tpy-Pm-R)]$^{2+}$) **2** and the homoleptic ([Ru(tpy-Pm-R)$_2$]$^{2+}$) **3** ruthenium complexes were synthesized (Scheme 3). The heteroleptic ruthenium complexes **2** were obtained by heating ligands **1** with Ru(tpy)Cl_3 in ethanolic solutions followed by anion metathesis with NH_4PF_6. They were obtained in reasonable yields (69−91%), except for nitrile **1f** (35%), for which the cyano group may be susceptible to nucleophilic attack in alcoholic solution and in the presence of catalytically active Ru(III) and Ag(I).[21]

The homoleptic complexes **3** were synthesized by reaction of $RuCl_3$ hydrate and 2 equiv of ligands **1** in the presence of $AgNO_3$ in refluxing alcoholic solution, followed by chromatography and counteranion exchange with NH_4PF_6. The

(12) Fang, Y.-Q.; Taylor, N. J.; Hanan, G. S.; Loiseau, F.; Passalacqua, R.; Campagna, S.; Nierengarten, H.; Van, Dorsselaer, A. *J. Am. Chem. Soc.* **2002**, *124*, 7912.
(13) (a) Hassan, J.; Sévignon, M.; Gozzi, C.; Schulz, E.; Lemaire, M. *Chem. Rev.* **2002**, 1359 and references therein. (b) Farina, V.; Krishnamurthy, V.; Scott, W. J. *The Stille Reaction*; Wiley: New York, 1998. (c) Suzuki, A. *J. Organomet. Chem.* **1999**, *576*, 147.
(14) Pyridine ring-forming reactions: (a) Kröhnke, F. *Synthesis* **1976**, 1. (b) Constable, E. C.; Ward, M. D.; Corr, S. *Inorg. Chim. Acta* **1988**, *141*, 201. (c) Frank, R. L.; Riener, E. F. *J. Am. Chem. Soc.* **1950**, *72*, 4182. (d) Vaduvescu, S.; Potvin, P. G. *Eur. J. Inorg. Chem.* **2004**, 1763. (e) Wang, J.; Hanan, G. *Synlett* **2005**, 1251. Pyrimidine ring-forming reactions: Karpov, A. S.; Mueller, T. J. J. *Synthesis* **2003**, 2815. Bejan, E.; Haddou, H. Ait; Daran, J. C.; Balavoine, G. G. A. *Synthesis* **1996**, 1012. Ioachim, E.; Medlycott, E. A.; Polson, M. I. J.; Hanan, G. S. *Eur. J. Org. Chem.* **2005**, 3775.
(15) Goodall, W.; Wild, K.; Arm, K. J.; Williams, J. A. G. *J. Chem. Soc., Perkin Trans. 2* **2002**, 1669.
(16) Schaefer, F. C.; Peters, G. A. *J. Org. Chem.* **1961**, *26*, 412.
(17) Malhotra, S. S.; Whiting, M. C. *J. Chem. Soc.* **1960**, 3812.
(18) Arnold, Z.; Holy, A. *Collect. Czech. Chem. Commun.* **1963**, *28*, 2040.
(19) Davies, I. W.; Marcoux, J.-F.; Wu, J.; Palucki, M.; Corley, E. G.; Robbins, M. A.; Tsou, N.; Ball, R. G.; Dormer, P.; Larsen, R. D.; Reider, P. J. *J. Org. Chem.* **2000**, *65*, 4571.
(20) Kucera, J.; Arnold, Z. *Collect. Czech. Chem. Commun.* **1967**, *32*, 1704.
(21) (a) Gregson, S.; Shaw, G. *J. Chem. Soc., Perkin Trans. 1* **1985**, 187. (b) Wang, J.; Fang, Y.-Q.; Hanan, G. S.; Loiseau, F.; Campagna, S. *Inorg. Chem.* **2005**, *44*, 5.

Scheme 3. Preparation of Heteroleptic **2** and Homoleptic **3** Ru(II) Complexes of Ligands **1**

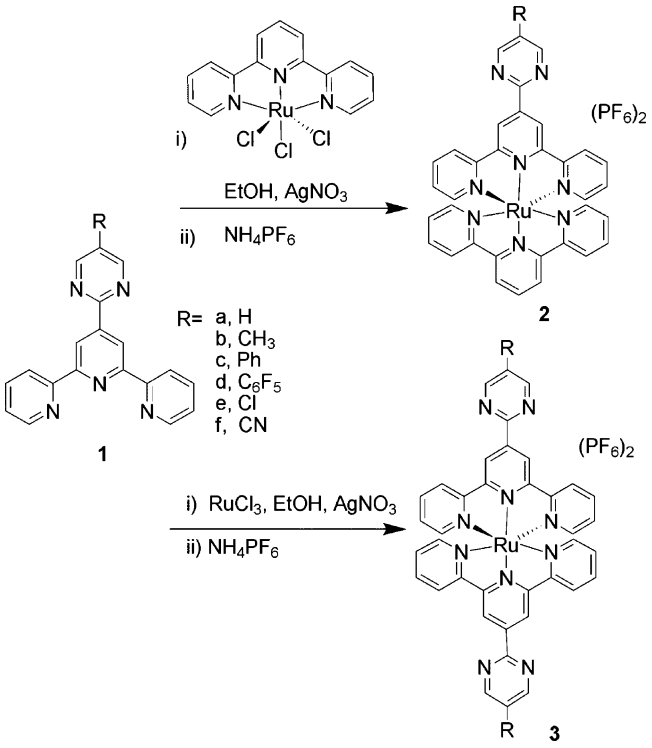

yields of the reactions are normally lower than those of the heteroleptic complexes (44−70%).

The solid-state structures of the ligand **1c** and complexes **2c** and **2d** were obtained by X-ray crystallography (Figure 3). Ligand **1c** was crystallized from ethanol by slow cooling of a hot saturated solution. Single crystals of complexes **2c** and **2d** were obtained as nitrate salts by the slow diffusion of di*iso*propyl ether vapor into a solution of [**2**]$(PF_6)_2$ and tetrabutylammonium nitrate in acetonitrile. It is found that

Table 1. Angles between Planes and Central Pyridine CH·to Pyrimidine N Distances for **1c**, **2c**, and **2d**

	1c		**2c**		**2d**	
Py-Pm (deg)[a]	6.6		4.5		8.8	
Pm−Ph (or F_5C_6) (deg)[b]	36.9		28.2		77.9	
CH−N distance (Å)	2.44	2.57	2.50	2.49	2.49	2.51

[a] Angle between the central pyridine and the pyrimidine ring. [b] Angle between the pyrimidine ring and the phenyl of pentafluorophenyl ring.

ligand **1c** was not solvated, whereas both the complexes were solvated by acetonitrile in the solid state. The experimental parameters are given in the Supporting Information.

Ligand **1c** adopts a *transoid*-conformation for the pyridine rings and the central pyridine to pyrimidine angle is low (6.6°), which favors both electronic conjugation and crystal packing (Table 1). In metal complexes **2c** and **2d**, the $[Ru(tpy)_2]^{2+}$ moieties adopt pseudooctahedral coordination spheres.[6] The bond lengths and angles about the Ru(II) centers are typical for $[Ru(tpy)_2]^{2+}$ complexes.

As expected,[22] all of the central pyridyl and the 2-pyrimidyl rings have very small angles between their planes (all under 10°) due to the absence of H···H repulsion, which dramatically contrasts to those between the 5-pyrimidyl rings and Ph or C_6F_5 (Table 1). In the case of C_6F_5, the size of the fluoro groups compounds the steric hindrance leading to a near orthogonal arrangement of the rings (77.9°). The distance between the pyrimidyl nitrogen atoms and the 3′,5′ protons on the tpy ligand are all about 2.50 Å, supporting weak CH−N hydrogen bonding as a contribution for the coplanarity between the heterocycles (Figure 3).

The electrochemical data were obtained in acetonitrile and are compiled in Table 2. The oxidation processes of Ru(II) polypyridine complexes are ascribed to metal-centered processes, whereas the reduction processes are ligand centered, in agreement with literature data and the reversibility of most of the processes.[2] As $[(Pm\text{-}tpy)Ru(tpy)]^{2+}$ (**2a**)

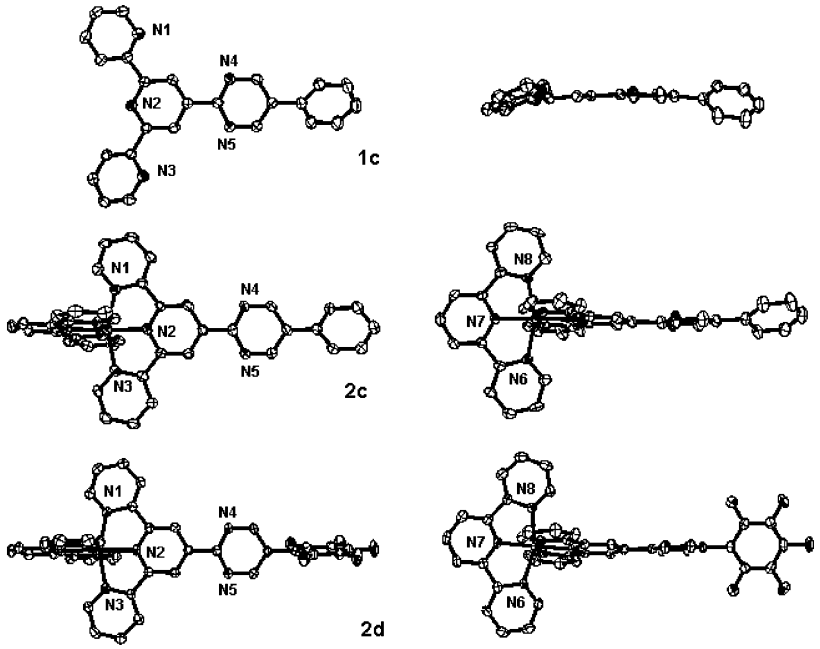

Figure 3. ORTEP plots of **1c**, **2c**, and **2d** at 30% probability, showing two orthogonal views for each crystal structure. The solvent and anions of crystallization are omitted for clarity.

Table 2. Redox Potential Data for Complexes **2** and **3**[a]

compd	$E_{1/2}$ (V) vs SCE (ΔE_p (mV) or irreversible)		
2a	1.32 (80)	−1.13 (70)	−1.48 (80)
2b	1.29 (60)	−1.15 (70)	−1.47 (110)
2c	1.31 (80)	−1.11 (70)	−1.46 (80)
2d	1.31 (60)	−1.04 (70)	−1.42 (90)
2e	1.33 (90)	−1.09 (60)	−1.46 (70)
2f	1.34 (75)	−0.92 (70)	−1.34 (70)
3a	1.33 (90)	−1.10 (70)	−1.32 (ir)
3b	1.31 (80)	−1.12 (65)	−1.38 (70)
3c	1.33 (90)	−1.07 (100)	−1.29 (100)
3d	1.35 (70)	−1.01 (70)	
3e	1.35 (80)	−1.05 (60)	−1.28 (ir)
3f	1.38 (60)	−0.89 (60)	−1.04 (70)
4[b]	1.30	−1.24	−1.49

[a] Scan rate 100 mV s^{-1}. $E_{1/2} = {}^1/_2(E_{pa} + E_{pc})$, where E_{pa} and E_{pc} are the anodic and cathodic peak potential respectively. $\Delta E_p = E_{pa} - E_{pc}$. ir = irreversible. Potentials are corrected by internal reference, ferrocene (395 mV). [b] **4** = $[Ru(tpy)_2]^{2+}$.[3b]

has almost the same oxidation potential as $[Ru(tpy)_2]^{2+}$, the introduction of the 2-pyrimidyl ring into the 4′-position of tpy has very little electronic effect on the ruthenium metal center as opposed to direct functionalization of the 4′-position of tpy.[6] Thus, the pyrimidyl groups have negligible effects on the metal-center (MC) orbitals, which allows functionalization of the ligands to tune the energy of the ligand-based π^*-orbital without disturbing (at a first approximation) the MC orbitals and states.

The reduction patterns are different for the homoleptic and heteroleptic complexes. As the heteroleptic complexes **2**, the first single-electron reduction involves the pyrimidyl-substituted ligand, and the second one is on nonsubstituted tpy moiety. In the heteroleptic complexes **3**, the first single-electron reduction occurs at a slightly less negative potential, by 30−40 mV, than in their heteroleptic analogues. The second reduction processes are also less negative than those of heteroleptic complexes as the second reduction occurs on another **1**-type ligand rather than tpy. The shift to less negative potentials of the first reduction of the **3** compounds compared to those of the corresponding **2** species is due to the presence of the second pyrimidyl-substituted terpy ligand. Such a "spectator" (with regard to the first reduction process) ligand is a better electron withdrawing group than tpy, and as consequence leaves less electron density on the ligand involved in the first reduction. Separation between first and second reduction in the **3** series is related to ligand−ligand coupling as mediated by the metal center and is roughly constant within the series.

The electronic properties pyrimidinyl of the substituents have more of an effect on the reduction potentials of the Pm-tpy moiety as compared to their effect on the metal center (see above). Electron-donating groups such as methyl destabilize the reduction process and electron-accepting groups such as the chloro group render the reductions more facile. This effect can be seen by plotting the redox potentials versus the σ_p Hammett parameter of the 5-pyrimidinyl group

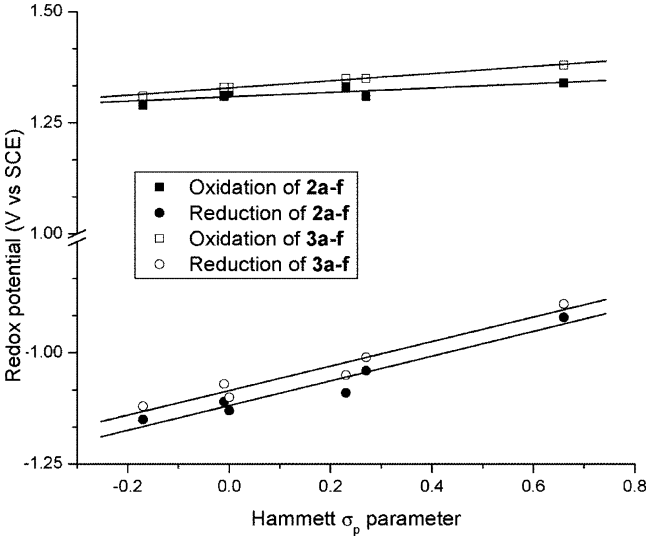

Figure 4. Plot of the redox potentials of complexes **2a**−**f** (solid circles and squares) and **3a**−**f** (empty circles and squares) vs the σ_p Hammett parameter of 5-pyrimidinyl substituent. The σ_p Hammett parameters for the various substituents are as follows:[23] 0 (H); −0.17 (CH_3); −0.01 (C_6H_5); 0.41 (C_6F_5); 0.23 (Cl); 0.66 (CN).

(Figure 4).[23] The reduction is facilitated by the electronegative substituents (Figure 4, bottom plot), whereas the oxidation potentials stay relatively constant through the series (Figure 4, top plot), confirming the negligible effect of the pyrimidinyl-substituents on the metal-centered oxidation potentials discussed previously. The electron delocalization ability of the 2-pyrimidinyl group can also be seen through its own σ_p parameter (0.53) which has a major contribution from resonance (0.40) and not induction (0.13), the latter being the main contributor for all of the R groups in Figure 4.[23]

Absorption Spectra and Photophysical Properties. The absorption and emission data of the new ruthenium species are gathered in Table 3, which also contains data for model complexes. For all of the compounds, the intense absorption bands in the visible region are assigned to spin-allowed metal-to-ligand charge-transfer (MLCT) transitions, whereas the absoption bands in the UV region are assigned to spin-allowed ligand-based $\pi \rightarrow \pi^*$ transitions. The molar absorption coefficients for complexes **2** and **3** are significantly larger than those of $[Ru(tpy)_2]^{2+}$ due to the greater number of heterocycles involved: the MLCT transitions in **2** and **3** extend over the (planar) pyrimidyl subtituents of the terpy ligands, leading to higher oscillator strength values. The absorption spectra of some representative compounds are shown in Figure 5.

All the complexes exhibit luminescence both at room temperature in fluid solution and at 77 K in rigid matrix (Table 3, Figure 5). Luminescence energy, lifetime, and quantum yields, together with energy emission shapes and the blue-shift of the emission on moving from room-temperature fluid solution to 77 K rigid matrix, clearly indicate that luminescence originates from the (formally) triplet MLCT state involving pyrimidine-substituted tpy

(22) An analysis of the Cambridge Crystallographic Database of the twist angles of 2-phenylpyrimidine (Ph-pm), 2-(2-pyridyl)-pyrimidine (py-pm), and biphenyl (Ph-Ph) supports a lower twist angle for Ph-pm as compared to py-pm and Ph-Ph; see Supporting Information.

(23) Hansch, C.; Leo, A.; Taft, R. W. *Chem. Rev.* **1991**, 91. 165.

Table 3. Spectroscopic and Photophysical Data in Deaerated CH_3CN Solutions, unless Otherwise Stated

		luminescence, 298 K					luminsecence, 77 K[a]	
compd	absorption λ_{max}, nm (ϵ, $M^{-1}\,cm^{-1}$)	λ_{max} nm	τ, ns	Φ ($\times 10^{-4}$)	k_r, s^{-1} ($\times 10^4$)	k_{nr}, s^{-1} ($\times 10^6$)	λ_{max}, nm	τ, μs
2a	273 (44100) 309 (43100) 486 (17300)	675	8	2.0	2.5	125.0	643	13.6
2b	274 (60900) 308 (55300) 484 (20600)	669	6	1.6	2.7	166.6	643	13.7
2c	272 (51600) 308 (73500) 489 (27900)	680	15	1.8	1.2	66.7	654	15.0
2d	274 (57700) 306 (56700) 488 (23800)	689	36	7.5	2.1	27.8	657	13.8
2e	274 (55500) 308 (55300) 487 (23700)	684	21	2.4	1.1	47.6	655	13.8
2f	275 (58400) 308 (48700) 497 (24800)	713	200	8.9	0.4	5.0	673	13.2
3a	276 (85500) 319 (64100) 494 (39200)	673	11	2.5	2.3	90.9	645	13.2
3b	283 (93600) 318 (70800) 494 (42000)	670	8	1.3	1.6	125.0	646	13.2
3c	285 (61000) 320 (75600) 496 (43100)	675	21	4.4	2.1	47.6	654	13.8
3d	286 (77900) 337 (55400) 500 (41400)	683	39	2.6	0.7	25.6	656	14.1
3e	284 (81000) 320 (52600) 495 (36600)	677	26	5.6	2.2	38.4	652	13.6
3f	287 (74300) 341 (49000) 506 (42000)	705	231	12.0	0.5	4.3	672	13.5
4[b]	474 (10400)	629	0.25	$\leq$0.05	0.4	90.9		
5[c]	487 (26200)	715	1.0	0.4				

[a] In butyronitrile rigid matrix. [b] **4** = $[Ru(tpy)_2]^{2+}$.[6] [c] **5** = $[Ru(Ph\text{-}tpy)_2]^{2+}$.[6]

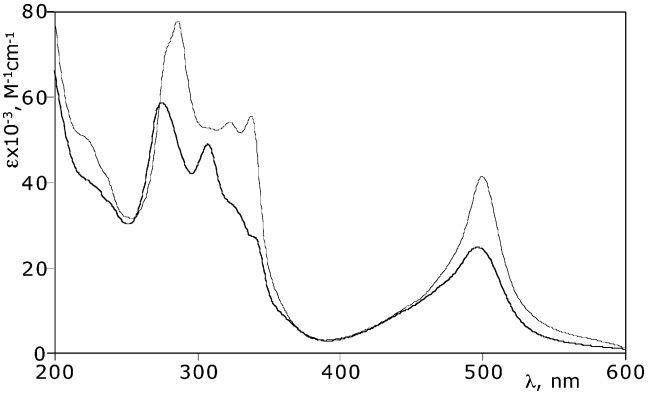

Figure 5. Absorption spectra of **2f** (bold line) and **3d** (solid line) in acetonitrile.

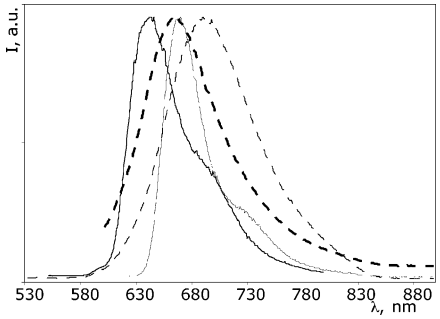

Figure 6. Luminescence spectra of **2a** (solid bold line, 77 K; dashed bold line, room temperature) and **3f** (solid line, 77 K; dashed line, room temperature). The spectra shown are not corrected for photomultiplier response, for corrected values, see Table 3.

ligand(s), as expected. The room-temperature lifetimes of all the **2** and **3** complexes are greater than that of **4** and **5** and increase with further substitution in the pyrimidine 5-position. The longest lifetimes belong to **2f** and **3f**, bearing the electron-withdrawing cyano group(s). Notably, the enhanced properties of the new complexes are obtained without too large a lowering of the excited-state energy (cf., **2a** vs **2f**).

To understand in detail the effect of the pyrimidine substituents, it is useful to recall that the excited-state lifetimes of Ru(II) polypyridine complexes are governed by the nonradiative decay rate constant k_{nr}, given by eq 1.[2,5]

$$k_{nr} = k_{nr}^{0} + k'_{nr} \quad (1)$$

The overall radiationless decay is the sum of two terms. The first one, k_{nr}^0, leads directly from the MLCT state to the

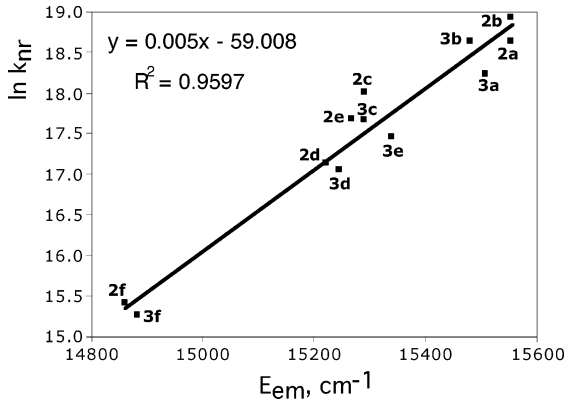

Figure 7. Plot of ln k_{nr} vs E_{em}^{max} for new complexes.

ground state, whereas the second term, k'_{nr}, is related to the thermally activated process that takes into account a surface-crossing from the lowest-lying MLCT state to a closely lying metal-centered (MC) level,[2,5] so it depends on the energy gap ΔE between MLCT and MC states (when coupling between these two states is relatively high). For Ru(II) complexes with tridentate ligands, the second term normally dominates the equation. The small ΔE between MLCT and MC states in Ru(II) tridentate polypyridine complexes, a consequence of the reduced ligand field strength experienced by the metal center compared to Ru(II) bidentate polypyridine ligands, due to an ill-fitted octahedral arrangement, is in fact responsible for the poor room-temperature luminescence properties of $Ru(tpy)_2$-type complexes, as already mentioned in the Introduction.[2,5b]

On plotting log k_{nr}, versus E_{em}^{max}, a linear relationship with a positive slope is obtained (Figure 7).[24] This finding, which contrasts the energy gap law,[2a,24] confirms that the dominant term for k_{nr} in the series of complexes here investigated is the second term of eq 1. Indeed, the MC level energy can be considered as a constant within the series, whereas the MLCT emitting level decreases in energy with the electron withdrawing ability of the substituents on the pyrimidines. Therefore, this linear relationship expresses the reduced efficiency of the MLCT-to-MC surface-crossing pathway as the MLCT excited-state energy is decreased. The expected variation of k_{nr}^0 on MLCT excited-state energy is evidently too subtle within the series to alter the linearity of the relationship.

However, the larger energy gap between MLCT and MC states is not enough to fully justify the (relatively) long luminescence lifetimes of the complexes, as for example clearly showed by comparing data of **2f** and **5** (Table 3). These latter complexes exhibit very close room-temperature luminescence maxima (713 vs 715 nm) but have quite different lifetimes (200 vs 1 ns, respectively). Similar results are obtained when comparing the luminescence lifetimes of complexes **2** and **3** with those of analogous $[Ru(tpy_2]$-like species missing the pyrimidine subunit(s).[3b] This suggests that the effect on k'_{nr} is not the only one produced by the pyrimidine substituents. The additional effect has to be found in the k_{nr}^0 term, which depends on the electronic coupling between ground and MLCT states.

Estimates of the coupling between ground and emitting states can be obtained by spectral fitting of the emission profile, following eq 2:[25−29]

$$L(\bar{\nu}) = \sum_{x=0}^{5}\left[\left(\frac{E_0 - x\hbar\omega}{E_0}\right)^3\left(\frac{S^x}{x!}\right)\times \left(\left[\exp\left[-4\ln 2\left(\frac{\bar{\nu} - E_0 + x\hbar\omega}{\Delta\nu_{1/2}}\right)^2\right]\right]\right] \quad (2)$$

In eq 2, $L(\bar{\nu})$ is the relative emission intensity at energy $\bar{\nu}$, E_0 is the energy of the zero−zero transition (i.e., the energy of the emitting ^{3}MLCT state), $\hbar\omega$ is the average of medium frequency acceptor modes coupled to the MLCT transition, x is the quantum number of such an averaged medium-frequency mode which serves as the final vibronic states, $\Delta\nu_{1/2}$ is the half-width of the individual vibronic bands, and S is the Huang−Rhys factor, defined—for a homogeneous series of compounds—as in eq 3.[25−27]

$$S = \frac{1}{2}\left(\frac{2\pi M\omega}{h}\right)(\Delta Q)^2 \quad (3)$$

In eq 3, M is the reduced mass of the oscillator, ω is the dominant vibrational mode frequency, and ΔQ represents the difference between the ground- and excited-state equilibrium geometries with respect to the nuclear coordinates. The Huang−Rhys factor S gauges the electron-vibration coupling constant between ground and emitting states. Assuming roughly constant the $(h/2\pi)\omega$ value in a homogeneous series of complexes, a smaller value of S indicates a smaller degree of excited-state distortion related to the ground state along coordinates coupled to the excited-state relaxation.[25−29]

The parameter values obtained from the spectral fittings of the emission spectra for all the complexes at room temperature are listed in Table 4. It can be seen that for all the new complexes of both the **2** and **3** series, the Huang−Rhys factors are smaller than that reported for the parent compound 4 ($S = 0.7$). This result therefore indicates that a reduced ΔQ occurs in all the compounds compared to the model **4** species. This translates into a smaller Franck−

(24) (a) Englman, R.; Jortner, J. *J. Mol. Phys.* **1970**, *18*, 145. (b) Henry, B. R.; Siebrand, W. In *Organic Molecular Photophysics*; Birks, J. B., Ed.; Wiley: New York, 1973; Vol. 1. (c) Caspar, J. V.; Kober, E. M.; Sullivan, B. P.; Meyer, T. J. *J. Am. Chem. Soc.* **1982**, *104*, 630−632. (d) Chen, P.; Meyer, T. J. *Chem. Rev.* **1998**, *98*, 1439.

(25) (a) Caspar, J. V.; Meyer, T. J. *Inorg. Chem.* **1983**, *22*, 2444. (b) Caspar, J. V.; Meyer, T. J. *J. Am. Chem. Soc.* **1983**, *105*, 5583. (c) Claude, J. P.; Meyer, T. J. *J. Phys. Chem.* **1995**, *99*, 51, and references therein.

(26) Damrauer, N. H.; Boussie, T. R.; Devenney. M.; McCusker, J. K. *J. Am. Chem. Soc.* **1997**, *1997*, 8253.

(27) Treadway J. A.; Strouse, G. F.; Ruminski, R. R.; Meyer, T. J. *Inorg. Chem.* **2001**, *40*, 4508 and references therein.

(28) Hupp, J. T.; Neyhart, G. A.; Meyer, T. J.; Kober, E. M. *J. Phys. Chem.* **1992**, *96*, 10820.

(29) In this treatment, low-frequency modes (including the solvent) are treated classically as average armonic oscillators in the limit $\hbar\omega << kT$. This approximation allows for a reduction in the number of fitting parameters and allows each vibronic component to be described by a Gaussian distribution function. In this schematization, coupling to a single high-frequency vibrational mode (an average energy of the high-frequency modes coupling final and initial states) is considered.

Table 4. Fitting Parameters for the Room-Temperature Emission Spectra of the New Complexes, Obtained by Eq 2[a]

compd	S	$\Delta\nu$ (cm^{-1})	E^{00} (cm^{-1})	E_{em} 77 K (cm^{-1})
2a	0.26	2104	14779	15552
2b	0.38	1917	14930	15552
2c	0.41	1892	14716	15290
2d	0.23	1987	14483	15220
2e	0.25	2084	14573	15267
2f	0.50	1882	14081	14859
3a	0.43	1909	14899	15504
3b	0.49	2011	15135	15480
3c	0.29	2011	14812	15290
3d	0.51	1944	14768	15244
3e	0.44	1946	14806	15337
3f	0.26	1972	14195	14881

[a] In the fitting, $\Delta\nu$, E_{00}, and S are left as floating parameters and $(h/2\pi)\omega$ is fixed to 1600 cm^{-1}. The calculations were made by restricting the quantum number of the average medium-frequency vibrational mode (i.e., the x value of eq 2) to a maximum value of 5.

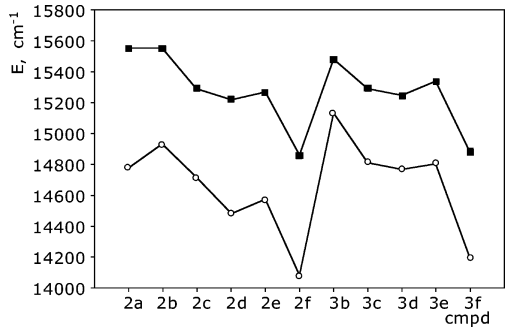

Figure 8. Comparison between calculated energy level of the MLCT state at room temperature and experimental emission energy at 77 K. Full squares: 77 K emission energy; empty circles: calculated room-temperature emission energy. For details, see text.

Condon (FC) factor for direct radiationless decay from the MLCT to the ground state and as a consequence to reduced k_{nr}^0 values for all the new complexes with respect to the parent **4** compound. A rough inspection of literature values allows for extending the comparison to other $[Ru(tpy)_2]^{2+}$-like complexes,[5b] and the same conclusions are obtained. The reduced value of S in **2** and **3** complexes is a direct consequence of a larger delocalization of the acceptor orbital of the MLCT transition[1g,8,12,25−28] involving ligands **1**, in agreement with the coplanarity between tpy and its pyrimidine substituents.

It can be noted that the energy of the emitting excited-state calculated by eq 2 is always lower than the corresponding experimental 77 K emission energy (see Table 4 and Figure 8). Such a difference, roughly constant within the series, would be related to the stabilizing effect of the solvent in fluid solution at room temperature; this effect is absent in rigid matrix at 77 K.

Conclusion

In conclusion, we introduced new pyrimidine-substituted terpyridine ligands and used them to prepare new Ru(II) polypyridine complexes. The metal complexes so obtained exhibit photophysical properties which are significantly better compared to those of $[Ru(tpy)_2]^{2+}$ and well comparable with the best emitters of Ru(II) polypyridine complexes containing tridentate ligands. Reasons for the improved photophysical properties lie at the same time in an enhanced MLCT-MC energy gap and in an increased delocalization in the acceptor ligand of the MLCT emitting excited states. The enhanced MLCT-MC energy gap leads to diminished efficiency of the thermally activated pathway for the radiationless process, whereas the increased delocalization in the acceptor ligand causes reduced Franck Condon factors for the direct radiationless decay from the MLCT state to the ground state of the new complexes in comparison with $[Ru(tpy)_2]^{2+}$ and similar species.

Because of their improved photophysical properties, the complexes here investigated hold promise to be suitable components for larger supramolecular (multicomponent) systems based on Ru(II) tridentate polypyridine compounds capable of performing long-range photoinduced electron and/or energy transfer functions.

Experimental Section

Materials and Instrumentation. 1H NMR, 13C NMR, and 19F NMR spectra were obtained using AVANCE AM-400 and AVANCE AMX-500 spectrometers. Melting points were collected using a MeltempTM 200 apparatus and are reported uncorrected. All reagents were used without further purification unless otherwise noted. 1H NMR assignments were made by determining the ring protons using 2D COSY experiments and then assigning the rings by NOE experiments based on the 3′,5′-singlet. All reactions were performed under a dry argon atmosphere using standard Schlenk or glove box techniques. Solvents for the reaction were predried using Pure-Solv Solvent Purification System (Innovative Technology Inc.). Palladium catalysts and phosphine ligands were purchased from STREM. All other chemicals were purchased from Sigma-Aldrich and used as received.

Absorption and emission spectra were measured in deaerated acetonitrile at room temperature on a Cary 500i UV−vis-NIR Spectrophotometer and a Jobin-Yvon Spex Fluoromax P (equipped with a Hamamatsu R3896 photomultiplier), respectively. Luminescence spectra have been corrected for photomultiplier response by using a program purchased with the fluorimeter. Luminescence lifetimes have been measured by an Edinburgh OB 900 time-correlated single-photon counting spectrometer employing a Hamamatsu PLP2 laser diode as pulse (wavelength output, 408 nm; pulse width, 59 ps). Emission quantum yields were measured at room-temperature using the optically dilute method.[30] $[Ru(bpy)_3]^{2+}$ in air-equilibrated aqueous solution was used as quantum yield standard ($\Phi = 0.028$).[31]

Electrochemistry data were collected in deaerated acetonitrile with 0.1 M Bu_4NPF_6 on a BAS CV-50W voltammetric analyzer. Redox potentials were corrected by the internal reference ferrocene (395 mV vs SCE).

Experimental uncertainties were as follows: absorption maxima, ±2 nm; molar absorption coefficients, 10%; emission maxima, ±5 nm; excited-state lifetimes, 10%; luminescence quantum yields, 20%; redox potentials, ±10 mV.

Synthesis. 4′-Terpyridylamidine Hydrochloride (7). 4′-Cyanoterpyridine (2.00 g, 7.7 mmol) and MeONa (0.062 g, 1.1 mmol) were added into dry methanol (150 mL), and the mixture was stirred at room temperature (occasionally warmed up to 40 °C to dissolve the starting material) for 12 h. Solid NH_4Cl (0.472 g, 8.8 mmol) was then added, and the mixture was stirred at room temperature

(30) Crosby, G. A.; Demas, J. N. *J. Phys. Chem.* **1971**, *75*, 991.
(31) Nakamaru, N. *Bull. Chem. Soc. Jpn.* **1982**, *55*, 2697.

for 2 d. Most of the solvent methanol was removed under vacuum until the solution was saturated (~50 mL). A large amount of diethyl ether (500 mL) was then added to precipitate the product. After filtration and washing with diethyl ether, the product was obtained as a white powder (2.05 g, 85%).

^{1}H NMR (300 MHz; DMSO-d_3) δ 8.80 (s, 2H), 8.73 (d, J=4.2 Hz, 2H), 8.61 (d, J=7.9 Hz, 2H), 8.52 (br, 1H), 8.00 (t, J=7.5 Hz, 2H), 7.76 (br, 1H), 7.50 (dd, J=6.6, 5.3 Hz, 2H). ^{13}C NMR (75 MHz; DMSO-d_6) δ 167.0, 156.2, 155.2, 149.9, 144.7, 138.1, 125.2, 121.5, 119.1.

Procedure for Ligands 1a−f as for Ligand 1a. 4′-(2-Pyrimidyl)-2,2′:6′,2″-terpyridine (1a). Vinamidine perchlorate (0.136 g, 0.6 mmol), 4′-terpyridylamidine (0.150 g, 0.48 mmol), and sodium methoxide (0.042 g, 0.78 mmol) were refluxed overnight in dry methanol (30 mL). The mixture was filtered, washed with chilled methanol (2 × 5 mL), and dried in vacuo to obtain a white crystalline product (0.045 g, 30%). mp 287.5−288.5 °C (methanol). ^{1}H NMR (300 MHz; $CDCl_3$) δ 9.42 (s, 2H, $H_{3',5'}$), 8.89 (d, J=4.9 Hz 2H, $H_{Pm,4,6}$), 8.74 (d, J=4.9 Hz, 2H, $H_{6,6''}$), 8.63 (d, J=7.9 Hz, 2H, $H_{3,3''}$), 7.84 (td, J^t=7.7 Hz, J^d=1.7 Hz, 2H, $H_{4,4''}$), 7.38 (ddd, J=7.5, 4.8, 1.0 Hz, 2H, $H_{5,5''}$), 7.29 (t, J=4.8 Hz, 1H, $H_{Pm,5}$). ^{13}C NMR (75 MHz; $CDCl_3$) δ 163.2, 157.5, 156.5, 156.2, 149.4, 147.2, 136.9, 123.9, 121.3, 120.6, 119.7. Anal. Calcd for $C_{19}H_{13}N_5$: C, 73.30; H, 4.21; N, 22.49. Found: C, 73.36; H, 4.13; N, 22.61.

4′-(5-Methyl-2-pyrimidyl)-2,2′:6′,2″-terpyridine (1b). Yield 76%. mp 259−260 °C (methanol). ^{1}H NMR (300 MHz; $CDCl_3$) δ 9.41 (s, 2H, $H_{3',5'}$), 8.74 (d, J=4.4 Hz 2H, $H_{6,6''}$), 8.71 (s, 2H, $H_{Pm,4,6}$), 8.63 (d, J=8.0 Hz, 2H, $H_{3,3''}$), 7.84 (t, J=7.8 Hz, 2H, $H_{4,4''}$), 7.38 (dd, J=7.0 Hz, 5.1 Hz, 2H, $H_{5,5''}$), 2.37 (s, 3H, Me). ^{13}C NMR (75 MHz; $CDCl_3$) δ 160.9, 157.6, 156.4, 156.3, 149.3, 147.3, 136.9, 130.1, 123.8, 121.3, 119.5, 15.8. Anal. Calcd for $C_{20}H_{15}N_5$: C, 73.83; H, 4.65; N, 21.52. Found: C, 74.02; H, 4.63; N, 22.64.

4′-(5-Phenyl-2-pyrimidyl)-2,2′:6′,2″-terpyridine (1c). Yield 85%. mp 246−247 °C (methanol). ^{1}H NMR (300 MHz; $CDCl_3$) δ 9.49 (s, 2H, $H_{3',5'}$), 9.10 (s, 2H, $H_{Pm,4,6}$), 8.76 (dd, J=4.0, 0.8 Hz, 2H, $H_{6,6''}$), 8.66 (d, J=8.0 Hz, 2H, $H_{3,3''}$), 7.87 (td, J^t=7.7 Hz, J^d=1.8 Hz, 2H, $H_{4,4''}$), 7.65 (d, J=7.0 Hz, 2H, Ph), 7.56−7.45 (m, 3H, Ph), 7.34 (ddd, J=7.4, 4.8, 1.1 Hz, 2H, $H_{5,5''}$). ^{13}C NMR (75 MHz; $CDCl_3$) δ 161.9, 156.5, 156.2, 155.4, 149.4, 146.9, 136.8, 134.4, 133.2, 129.5, 129.1, 127.1, 123.9, 121.3, 119.6. Anal. Calcd for $C_{25}H_{17}N_5$: C, 77.50; H, 4.42; N, 18.08. Found: C, 77.31; H, 4.40; N, 18.17.

4′-(5-Pentafluorophenyl-2-pyrimidyl)-2,2′:6′,2″-terpyridine (1d). Yield 76%. mp 274−275 °C (methanol). ^{1}H NMR (300 MHz; $CDCl_3$) δ 9.50 (s, 2H, $H_{3',5'}$), 9.01 (t, $^4J_{F-H}$=1.2 Hz, 2H, $H_{Pm,4,6}$), 8.76 (dd, J=4.8 Hz, 0.9 Hz, 2H, $H_{6,6''}$), 8.66 (d, J=8.0 Hz, 2H, $H_{3,3''}$), 7.88 (td, J^t=7.8 Hz, J^d=1.8 Hz, 2H, $H_{4,4''}$), 7.35 (ddd, J=7.3, 4.9, 0.9 Hz, 2H, $H_{5,5''}$). ^{19}F NMR (282 MHz; $CDCl_3$) δ 66.7 (dd, J=23, 8 Hz, 2F), −75.9 (t, J=21 Hz, 1F), −84.5 (td, J^t=24 Hz, J^d=7 Hz, 4F). Anal. Calcd for $C_{25}H_{12}F_5N_5$: C, 62.90; H, 2.53; N, 14.67. Found: C, 66.43; H, 3.47; N, 14.81.

4′-(5-Chloro-2-pyrimidyl)-2,2′:6′,2″-terpyridine (1e). Yield 76%. mp 231.5−233 °C (methanol). ^{1}H NMR (300 MHz; $CDCl_3$) δ 9.40 (s, 2H, $H_{3',5'}$), 8.84 (s, 2H, $H_{Pm,4,6}$), 8.75 (d, J=4.1 Hz, 2H, $H_{6,6''}$), 8.65 (d, J=7.9 Hz, 2H, $H_{3,3''}$), 7.86 (td, J^t=7.8 Hz, J^d=1.7 Hz, 2H, $H_{4,4''}$), 7.34 (ddd, J=7.3, 4.9, 0.8 Hz, 2H, $H_{5,5''}$). ^{13}C NMR (75 MHz; $CDCl_3$) δ 161.0, 156.6, 156.0, 156.0, 149.4, 145.9, 136.9, 131.0, 124.0, 121.3, 119.5. Anal. Calcd for $C_{19}H_{12}ClN_5$: C, 66.00; H, 3.50; N, 20.25. Found: C, 66.14; H, 3.45; N, 20.43.

4′-(5-Cyano-2-pyrimidyl)-2,2′:6′,2″-terpyridine (1f). Yield 67%. mp 284 °C (dec). ^{1}H NMR (300 MHz; $CDCl_3$) δ 9.42 (s, 2H, $H_{3',5'}$), 9.11 (s, 2H, $H_{Pm,4,6}$), 8.74 (dt, J^d=4.0 Hz, J^t=0.8 Hz, 2H, $H_{6,6''}$), 8.64 (d, J=7.9 Hz, 2H, $H_{3,3''}$), 7.87 (td, J^t=7.7 Hz, J^d=1.8 Hz, 2H, $H_{4,4''}$), 7.38 (ddd, J=7.4, 4.9, 1.0 Hz, 2H, $H_{5,5''}$). ^{13}C NMR (75 MHz; $CDCl_3$) δ 164.9, 160.0, 156.9, 155.7, 149.5, 145.0, 137.0, 124.2, 121.4, 119.9, 114.7, 108.6. Anal. Calcd for $C_{20}H_{12}N_6$: C, 71.42; H, 3.60; N, 24.99. Found: C, 71.42; H, 3.45; N, 25.17.

Procedure for Heteroleptic Ruthenium Complexes 2a−f as for Complex 2a. (Pmtpy)Ru(tpy) $(PF_6)_2$ (2a). 4′-(2-Pyrimidyl)-terpyridine (0.063 g, 0.2 mmol), ruthenium terpyridine trichloride (0.089 g, 0.2 mmol), and silver nitrate (0.104 g, 0.6 mmol) were refluxed overnight in ethanol (30 mL). The mixture was filtered through Celite, and the filtrate was evaporated to dryness. The residue was then chromatographed on a silica gel column with 7:1 acetonitrile and saturated aqueous KNO_3. Anion exchange with NH_4PF_6 gave pure **2a** (0.169 g, 89%).

^{1}H NMR (500 MHz; CD_3CN) δ 9.69 (s, 2H, $H_{3',5'}$), 9.15 (d, J=4.8 Hz, 2H, $H_{Pm,4,6}$), 8.78 (d, J=8.2 Hz, 2H, $H_{3',5'}$), 8.69 (d, J=8.1 Hz, 2H, $H_{3,3''}$), 8.51 (d, J=8.1 Hz, 2H, $H_{3,3''}$), 8.45 (t, J= 8.2 Hz, 1H, $H_{4'}$), 7.96 (td, J^t=8.0 Hz, J^d=1.1 Hz, 2H, $H_{4,4''}$), 7.92 (td, J^t=8.1 Hz, J^d=1.2 Hz, 2H, $H_{4,4''}$), 7.65 (t, J^t= 4.9 Hz, 1H, H_{Pm5}), 7.41 (d, J=5.6 Hz, 2H, $H_{6,6''}$), 7.39 (d, J=5.6 Hz, 2H, $H_{6,6''}$), 7.21 (td, J^t=6.6 Hz, J^d=1.0 Hz, 2H, $H_{5,5''}$), 7.15 (td, J^t=6.6 Hz, J^d=1.0 Hz, 2H, $H_{5,5''}$). ^{13}C NMR (75 MHz; CD_3CN) δ 161.1, 158.5, 158.0, 158.0, 156.0, 155.2, 152.6, 152.5, 144.8, 138.3, 138.2, 136.2, 127.7, 127.5, 124.8, 124.5, 123.9, 122.0, 121.6. Anal. Calcd for $C_{34}H_{24}F_{12}N_8P_2Ru\cdot H_2O$: C, 42.82; H, 2.75; N, 11.75. Found: C, 42.69; H, 2.74; N, 11.81. ESI-MS: 791.3 ([(Pmtpy)Ru(tpy) $(PF_6)]^+$), 323.0 ([(Pmtpy)Ru(tpy)]$^{2+}$).

(MePmtpy)Ru(tpy)$(PF_6)_2$ (2b). Yield 91%. ^{1}H NMR (500 MHz; CD_3CN) δ 9.67 (s, 2H, $H_{3',5'}$), 8.98 (s, 2H, $H_{Pm,4,6}$), 8.77 (d, J=8.2 Hz, 2H, $H_{3'5'}$), 8.68 (d, J=8.1 Hz, 2H, $H_{3,3''}$), 8.51 (d, J=8.1 Hz, 2H, $H_{3,3''}$), 8.44 (t, J=8.2 Hz, 1H, $H_{4'}$), 7.96 (td, J^t=7.4 Hz, J^d=1.1 Hz, 2H, $H_{4,4''}$), 7.93 (td, J^t=7.4 Hz, J^d=1.1 Hz, 2H, $H_{4,4''}$), 7.41 (d, J=5.3 Hz, 2H, $H_{6,6''}$), 7.38 (d, J=5.3 Hz, 2H, $H_{6,6''}$), 7.20 (ddd, J=6.9, 6.2, 1.0 Hz, 2H, $H_{5,5''}$), 7.15 (ddd, J=7.0, 6.2, 1.0 Hz, 2H, $H_{5,5''}$), 2.51(s, 3H, Me). ^{13}C NMR (75 MHz; CD_3CN) δ 158.6, 158.4, 158.0, 158.0, 155.9, 155.2, 152.6, 152.5, 145.0, 138.2, 138.2, 136.1, 132.4, 127.6, 127.5, 124.8, 124.5, 123.8, 121.4, 15.0. Anal. Calcd for $C_{35}H_{26}F_{12}N_8P_2Ru$: C, 44.27; H, 2.76; N, 11.80. Found: C, 43.97; H, 2.94; N, 11.89. ESI-MS: 805.1 ([(MePmtpy)Ru(tpy) $(PF_6)]^+$), 330.1 ([((MePmtpy)Ru(tpy)]$^{2+}$).

(PhPmtpy)Ru(tpy) $(PF_6)_2$ (2c). Yield 69%. ^{1}H NMR (500 MHz; CD_3CN) δ 9.73 (s, 2H, $H_{3',5'}$), 9.42 (s, 2H, $H_{Pm,4,6}$), 8.79 (d, J=8.2 Hz, 2H, $H_{3',5'}$), 8.72 (d, J=8.0 Hz, 2H, $H_{3,3''}$), 8.52 (d, J=8.1 Hz, 2H, $H_{3,3''}$), 8.46 (t, J=8.2 Hz, 1H, $H_{4'}$), 7.97 (td, J^t=8.0 Hz, J^d=1.0 Hz, 2H, $H_{4,4''}$), 7.95 (d, J=7.2 Hz, 2H, $H_{Ph,2,6}$), 7.93 (td, J^t=7.8 Hz, J^d=1.0 Hz, 2H, $H_{4,4''}$), 7.67 (t, J=7.5 Hz, 2H, $H_{Ph,3,5}$), 7.60 (t, J=7.4 Hz, 1H, $H_{Ph,4}$), 7.44 (d, J=5.6 Hz, 2H, $H_{6,6''}$), 7.40 (d, J=5.2 Hz, 2H, $H_{6,6''}$), 7.22 (ddd, J=7.2, 6.0, 1.0 Hz, $H_{5,5''}$, 2H), 7.15 (ddd, J=7.6, 5.6, 1.1 Hz, $H_{5,5''}$, 2H). ^{13}C NMR (75 MHz; CD_3CN) δ 159.7, 158.0, 158.0, 156.1, 156.0, 155.2, 152.6, 152.5, 144.4, 138.3, 138.2, 136.2, 134.0, 133.9, 129.6, 127.7, 127.5, 127.4, 124.9, 124.6, 123.9, 121.5. Anal. Calcd for $C_{40}H_{28}F_{12}N_8P_2Ru\cdot H_2O$: C, 46.66; H, 2.94; N, 10.88. Found: C, 46.68; H, 3.01; N, 10.68. ESI-MS: 867.1 ([(PhPmtpy)Ru(tpy)$(PF_6)]^+$), 361.2 ([((PhPmtpy)Ru(tpy)]$^{2+}$).

(F_5PhPmtpy)Ru(tpy) $(PF_6)_2$ (2d). Yield 80%. ^{1}H NMR (500 MHz; CD_3CN) δ 9.73 (s, 2H, $H_{3',5'}$), 9.29 (s, 2H, $H_{Pm,4,6}$), 8.79 (d, J=8.2 Hz, 2H, $H_{3',5'}$), 8.72 (d, J=8.1 Hz, 2H, $H_{3,3''}$), 8.52 (d, J=8.1 Hz, 2H, $H_{3,3''}$), 8.46 (t, J= 8.2 Hz, 1H, $H_{4'}$), 7.98 (td, J^t=7.9 Hz, J^d=1.3 Hz, 2H, $H_{4,4''}$), 7.94 (td, J^t=7.9 Hz, J^d=1.3 Hz, 2H, $H_{4,4''}$), 7.42 (d, J=5.7 Hz, 2H, $H_{6,6''}$), 7.41 (d, J=5.7 Hz, 2H, $H_{6,6''}$), 7.23 (ddd, J=7.5, 5.7, 1.1 Hz, 2H, $H_{5,5''}$), 7.15 (ddd, J=7.5, 5.7, 1.1 Hz, 2H, $H_{5,5''}$). ^{13}C NMR (75 MHz; CD_3CN) δ 161.4, 158.7 (br), 158.0, 157.9, 156.1, 155.1, 152.7, 152.5, 143.8, 138.3, 138.2, 136.3, 127.8, 127.5, 124.9, 124.6, 123.9, 121.8. ^{19}F NMR (282 MHz; CD_3CN) δ

2.7 (d, J_{P}−F=707 Hz, 12F), −68.4 (dd, *J*=21, 8 Hz, 2F), −78.5 (t, *J*=20 Hz, 1F), −87.7 (td, J^t=21 Hz, J^d=6.8 Hz, 2F). Anal. Calcd for $C_{40}H_{23}F_{17}N_8P_2Ru$: C, 43.61; H, 2.10; N, 10.17. Found: C, 43.42; H, 2.04; N, 10.23. ESI-MS: 957.0 ([$(F_5C_6Pmtpy)Ru(tpy)(PF_6)]^+$), 406.1 ([$((F_5C_6Pmtpy)Ru(tpy)]^{2+}$).

(ClPmtpy)Ru(tpy) $(PF_6)_2$ (2e). Yield 69%. ^{1}H NMR (500 MHz; CD_3CN) δ 9.63 (s, 2H, $H_{3',5'}$), 9.15 (s, 2H, $H_{Pm,4,6}$), 8.78 (d, *J*=8.2 Hz, 2H, $H_{3',5'}$), 8.69 (d, *J*=8.0 Hz, 2H, $H_{3,3''}$), 8.51 (d, *J*=8.1 Hz, 2H, $H_{3,3''}$), 8.45 (t, *J*=8.2 Hz, $H_{4'}$, 1H), 7.96 (td, J^t=7.6 Hz, J^d=1.3 Hz, 2H, $H_{4,4''}$), 7.93 (td, J^t=8.0 Hz, J^d=1.2 Hz, $H_{4,4''}$, 2H), 7.40 (d, *J*=5.3 Hz, 2H, $H_{6,6''}$), 7.39 (d, *J*=4.7 Hz, 2H, $H_{6,6''}$), 7.21 (ddd, *J*=7.8, 5.4, 1.1 Hz, 2H, $H_{5,5''}$), 7.15 (ddd, *J*=7.8, 5.4, 1.1 Hz, $H_{5,5''}$, 2H). ^{13}C NMR (75 MHz; CD_3CN) δ 159.1, 158.0, 157.9, 157.0, 156.1, 155.1, 152.7, 152.5, 143.5, 138.3, 138.2, 136.3, 132.0, 127.7, 127.5, 124.9, 124.6, 123.9, 121.6. Anal. Calcd for $C_{34}H_{27}ClF_{12}N_8O_2P_2Ru\cdot1.5H_2O$: C, 40.96; H, 2.63; N, 11.24. Found: C, 41.27; H, 2.69; N, 11.18. ESI-MS: 825.0 ([(ClPmtpy)Ru(tpy) $(PF_6)]^+$), 340.2 ([(ClPmtpy)Ru(tpy)]$^{2+}$).

(CNPmtpy)Ru(tpy) $(PF_6)_2$ (2f). Yield 35%. ^{1}H NMR (500 MHz; CD_3CN) δ 9.68 (s, 2H, $H_{3',5'}$), 9.45 (s, 2H, $H_{Pm,4,6}$), 8.78 (d, *J*=8.2 Hz, 2H, $H_{3',5'}$), 8.71 (d, *J*=8.0 Hz, 2H, $H_{3,3''}$), 8.51 (d, *J*=8.1 Hz, 2H, $H_{3,3''}$), 8.47 (t, *J*=8.2 Hz, 1H, $H_{4'}$), 7.97 (td, J^t=7.9 Hz, J^d=1.4 Hz, 2H, $H_{4,4''}$), 7.93 (td, J^t=7.9 Hz, J^d=1.4 Hz, 2H, $H_{4,4''}$), 7.40 (d, *J*=5.7 Hz, 2H, $H_{6,6''}$), 7.38 (d, *J*=5.7 Hz, 2H, $H_{6,6''}$), 7.23 (ddd, *J*=7.6, 5.6, 1.2 Hz, 2H, $H_{5,5''}$), 7.14 (ddd, *J*=7.7, 5.6, 1.2 Hz, 2H, $H_{5,5''}$). ^{13}C NMR (75 MHz; CD_3CN) δ 162.6, 161.4, 157.9, 157.8, 156.3, 155.0, 152.7, 152.5, 142.5, 138.4, 138.3, 136.5, 127.8, 127.5, 125.0, 124.6, 123.9, 122.1, 114.9, 109.4. Anal. Calcd for $C_{35}H_{23}F_{12}N_9P_2Ru\cdot1.5H_2O$: C, 42.56; H, 2.65; N, 12.76. Found: C, 42.28; H, 2.30; N, 12.36. ESI-MS: 816.6 ([(CNPmtpy)Ru(tpy)-$(PF_6)]^+$), 336.0 ([(CNPmtpy)Ru(tpy)]$^{2+}$).

Procedure for Homoleptic Ruthenium Complexes 3a−f as for Complex 3b. Ru(tpyPmMe)$_2$ $(PF_6)_2$ (3b). Ligand 4′-(5-methyl-2-pyrimidyl)terpyridine **1b** (0.101 g, 0.31 mmol), ruthenium trichloride hydrate (0.035 g, 0.155 mmol), and silver nitrate (0.079 g, 0.466 mmol) were refluxed overnight in ethanol (50 mL). The mixture was filtered through Celite, and the filtrate was evaporated to dryness. The residue was then chromatographed on a silica gel column with 10:1 acetonitrile and saturated aqueous KNO_3. Anion exchange with NH_4PF_6 gave pure product (0.113 g, 70%). ^{1}H NMR (500 MHz; CD_3CN) δ 9.68 (s, 4H, $H_{3',5'}$), 8.99 (s, 4H, $H_{Pm,4,6}$), 8.69 (d, *J*=8.1 Hz, 4H, $H_{3,3''}$), 7.96 (td, J^t=7.9 Hz, J^d=1.5 Hz, 4H, $H_{4,4''}$), 7.45 (d, *J*=5.5 Hz, 4H, $H_{6,6''}$), 7.19 (ddd, *J*=7.5, 5.7, 1.3 Hz, 4H, $H_{5,5''}$), 2.52 (s, 6H, Me). ^{13}C NMR (75 MHz; CD_3CN) δ 158.6, 158.4, 158.0, 155.7, 152.6, 145.3, 138.3, 132.4, 127.6, 124.9, 121.4, 15.0. Anal. Calcd for $C_{40}H_{30}F_{12}N_{10}P_2Ru\cdot1.5H_2O$: C, 44.95; H, 3.11; N, 13.11. Found: C, 45.00; H, 3.38; N, 12.60. ESI-MS: 396.2 ([(MePmtpy)Ru(tpyPmMe)]$^{2+}$).

Ru(tpy-Pm−H)$_2$ $(PF_6)_2$ (3a). Yield: 32%. ^{1}H NMR (400 MHz, CD_3CN) δ ppm 9.70 (s, 2H, $H_{5',3'}$), 9.15 (d, *J*=4.9 Hz, 2H, $H_{Pm,4,6}$), 8.69 (ddd, *J*=0.73, 1.2, 8.2 Hz, 2H, $H_{3,3''}$), 7.96 (dt, J^t=8.1 Hz, J^d=1.5 Hz, 2H, $H_{4,4''}$), 7.66 (t, *J*=4.9 Hz, 1H, H_{Pm5}), 7.44 (ddd, *J*=0.64, 1.3, 5.6 Hz, 2H, $H_{6,6''}$), 7.18 (ddd, *J*=1.3, 5.6, 7.5 Hz, 2H, $H_{5,5''}$). ^{13}C (300 MHz, CD_3CN) δ 161.8, 159.3, 158.7, 156.5, 153.4, 145.9, 139.1, 128.5, 125.7, 122.8, 122.5. Anal. Calcd for $C_{38}H_{26}F_{12}N_{10}P_2Ru\cdot3H_2O$: C, 42.75; H, 3.02; N, 13.12. Found: C, 42.92; H, 2.85; N, 13.16. ES-MS: *m*/*z* = 869.1 ([(HPmtpy)Ru-(HPmtpy)$(PF_6)]^+$), 362.07 ([(HPmtpy)Ru(HPmtpy)]$^{2+}$).

Ru(PhPmtpy)$_2$ $(PF_6)_2$ (3c). Yield: 53%. ^{1}H NMR (500 MHz; CD_3CN) δ 9.76 (s, 4H, $H_{3',5'}$), 9.43 (s, 4H, $H_{Pm,4,6}$), 8.74 (d, *J*=8.1 Hz, 4H, $H_{3,3''}$), 7.98 (td, J^t=8.0 Hz, J^d=1.2 Hz, 4H, $H_{4,4''}$), 7.96 (d, *J*=7.2 Hz, 4H, $H_{Ph2,6}$), 7.68 (t, *J*=7.5 Hz, 4H, $H_{Ph3,5}$), 7.61 (t, *J*=7.4 Hz, 2H, $H_{Ph,4}$), 7.48 (d, *J*=5.6 Hz, 4H, $H_{6,6''}$), 7.21 (ddd, *J*=7.1, 6.0, 1.0 Hz, 4H, $H_{5,5''}$). ^{13}C NMR (75 MHz; CD_3CN) δ 159.7, 158.0, 156.1, 155.8, 152.7, 144.8, 138.4, 134.1, 133.9, 129.6, 127.7, 127.4, 125.0, 121.6. Anal. Calcd for $C_{50}H_{34}F_{12}N_{10}P_2Ru\cdot3H_2O$: C, 49.23; H, 3.30; N, 11.48. Found: C, 49.21; H, 3.11; N, 11.34. ESI-MS: 1021.2 ([(PhPmtpy)Ru(PhPmtpy) $(PF_6)]^+$), 438.2 ([((PhPmtpy)Ru-(PhPmtpy)]$^{2+}$).

Ru(tpyPmC_6F_5)$_2$ $(PF_6)_2$ (3d). Yield: 64%. ^{1}H NMR (500 MHz; CD_3CN) δ 9.75 (s, 4H, $H_{3',5'}$), 9.30 (s, 4H, $H_{Pm,4,6}$), 8.73 (d, *J*=8.0 Hz, 4H, $H_{3,3''}$), 7.99 (td, J^t=7.9 Hz, J^d=1.3 Hz, 4H, $H_{4,4''}$), 7.46 (d, *J*=4.9 Hz, 4H, $H_{6,6''}$), 7.21 (ddd, *J*=7.5, 5.7, 1.1 Hz, 4H, $H_{5,5''}$). ^{13}C NMR (75 MHz; CD_3CN) δ 161.3, 158.8, 157.8, 155.9, 152.7, 144.2, 138.4, 127.8, 125.0, 122.1, 121.9. (Peaks from F_5Ph are broad). ^{19}F NMR (282 MHz; CD_3CN) δ 2.6 (d, J_{P-F}=707 Hz, 12F), −68.4 (dd, *J*=22, 7 Hz, 4F), −78.4 (t, *J*=20 Hz, 2F), −87.7 (td, J^t=21 Hz, J^d=7 Hz, 4F). Anal. Calcd for $C_{50}H_{24}F_{22}N_{10}P_2Ru\cdot H_2O$: C, 44.03; H, 1.92; N, 10.27. Found: C, 44.23; H, 2.20; N, 10.11. ESI-MS: 528.2 ([$(F_5C_6Pmtpy)Ru(tpyPmC_6F_5)]^{2+}$).

Ru(ClPmtpy)$_2$ $(PF_6)_2$ (3e). Yield: 44%. ^{1}H NMR (500 MHz; CD_3CN) δ 9.66 (s, 4H, $H_{3',5'}$), 9.16 (s, 4H, $H_{Pm,4,6}$), 8.71 (d, *J*=8.1 Hz, 4H, $H_{3,3''}$), 7.97 (td, J^t=7.9 Hz, J^d=1.3 Hz, 4H, $H_{4,4''}$), 7.44 (d, *J*=4.9 Hz, 4H, $H_{6,6''}$), 7.19 (ddd, *J*=7.5, 5.7, 1.2 Hz, 4H, $H_{5,5''}$). ^{13}C NMR (75 MHZ; CD_3CN) δ 159.0, 157.8, 157.0, 155.8, 152.7, 143.9, 138.4, 132.1, 127.7, 125.0, 121.7. Anal. Calcd for $C_{38}H_{24}Cl_2F_{12}N_{10}P_2Ru\cdot2H_2O$: C, 40.80; H, 2.52; N, 12.52. Found: C, 40.95; H, 2.50; N, 12.19. ESI-MS: 937.1 ([(ClPmtpy)Ru(ClPmtpy) $(PF_6)]^+$), 396.2 ([(ClPmtpy)Ru(ClPmtpy)]$^{2+}$).

Ru(CNPmtpy)$_2$ $(PF_6)_2$ (3f). Yield: 33%. ^{1}H NMR (400 MHz, CD_3CN) δ ppm 9.70 (s, 1H, H $_{5',3'}$), 9.46 (s, 1H, $H_{Pm,4,6}$), 8.72 (d, *J*=8.31 Hz, 1H, $H_{3,3''}$), 7.97 (dt, *J*=8.02, 7.92, 1.16 Hz, 1H, $H_{4,4''}$), 7.42 (dd, *J*=5.48, 0.69 Hz, 1H, $H_{6,6''}$), 7.19 (ddd, *J*=7.32, 5.67, 1.04 Hz, 1H, $H_{5,5''}$). ^{13}C (300 MHz, CD_3CN): δ 163.4, 162.3, 158.5, 156.7, 153.5, 144.0, 139.3, 128.7, 126.0, 123.0, 115.7, 110.4. Anal. Calcd for $C_{40}H_{24}F_{12}N_{12}P_2Ru$ $2H_2O$ C, 43.69; H, 2.57; N, 15.28. Found: C, 43.43; H, 2.74; N, 14.52 ES-MS: *m*/*z* = 387.06 ([(CNPmtpy)Ru(CNPmtpy)]$^{2+}$).

Acknowledgment. G.S.H. thanks the NSERC (Canada) and the Université de Montréal for funding. S.C. thanks the University of Messina for funding. F.L. thanks the MIUR-FIRB project (contract no. RBNE019H9K) for a fellowship grant. Johnson Matthey is thanked for a loan of $RuCl_3$.

Supporting Information Available: Crystallographic data in CIF format for **1c**, **2c**, and **2d**, NMR spectra, twist angle analysis from data in the Cambridge Crystallographic Database, and crystallographic parameters. This material is available free of charge via the Internet at http://pubs.acs.org.

IC0622609